ChemComm

Mesoporous Sn–TiO_2 composite electrodes for lithium batteries

Zuoyan Peng, Zhong Shi and Meilin Liu*

School of Materials Science and Engineering, Georgia Institute of Technology, Atlanta, GA, 30332-0245SA. E-mail: meilin.liu@mse.gatech.edu

Received (in Irvine, CA, USA) 9th May 2000, Accepted 12th September 2000
First published as an Advance Article on the web 11th October 2000

Mesoporous TiO_2 is prepared stable up to 500 °C with BET surface area of 603 $m^2\ g^{-1}$ and pore size 6.9 nm, and Sn–TiO_2 composites based on the mesoporous TiO_2 show good potential as an electrode for lithium batteries with large capacity and structural integrity.

Since mesoporous materials (*e.g.* MCM-41) were first prepared in 1992,[1,2] surfactant-templated synthesis procedures have been widely used for the preparation of highly-ordered mesoporous or nanostructured materials which would be difficult to prepare otherwise. The ordering in these materials is a consequence of a self-assembly process in an aqueous solution containing organic surfactants (anionic, cationic or neutral) and inorganic (oligo-) cations or anions. A wide range of mesoporous materials have been prepared using the structure-directing functions of electrostatic, hydrogen-bonding, and van der Waals interactions associated with amphiphilic molecules.[3–14] Mesoporous TiO_2 was first prepared using a phosphate surfactant through a modified sol–gel process.[13] Since a significant amount of phosphorus still remained in these materials, they are not pure titanium oxides. Recently, mesoporous TiO_2 has been prepared using amphiphilic poly(alkylene oxide) block copolymers as structure-directing agents and titanium inorganic salts as precursors in a non-aqueous solution.[15] The mesoporous structure was stable up to 400 °C with BET (Brunauer–Emmett–Teller) surface area of about 200 $m^2\ g^{-1}$. The use of amine surfactants resulted in mesoporous TiO_2 with BET surface area about 700 $m^2\ g^{-1}$ (for as-synthesized powders) while heat treatment of the obtained materials in dry air at 300 °C led to loss of surface area and disappearance of the low angle diffraction peak in X-ray diffraction (XRD) patterns.[16] In this study, mesoporous TiO_2 stable up to 500 °C has been successfully prepared using tri-block copolymers, $(EO)_n$–$(PO)_m$–$(EO)_n$, as directing agents and titanium butoxide as precursor in an aqueous solution. Further, tin oxide was introduced into the mesoporous TiO_2 using a sol–gel process and then reduced in an atmosphere containing hydrogen to form a Sn–TiO_2 composite electrode for lithium ion batteries. The objective of our study is to create a nano-structured Sn–TiO_2 electrode for lithium ion batteries because tin-based compounds may offer much larger capacity than a lithiated carbon electrode. The structural stability of the tin-based materials during cycling is a major concern.[17] Our approach to improve the structural stability was to incorporate tin compound into a mesoporous TiO_2 matrix, which is structurally stable and hence offers structural stability to the nanocomposite electrode.

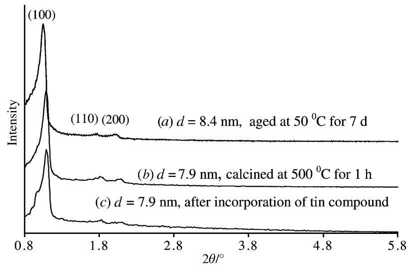

Fig. 1 XRD patterns of (*a*) as-synthesized (aged at 50 °C for 1 week) and (*b*) as-calcined (at 500 °C in air for 1 h) TiO_2 samples prepared using Pluronic 103 as surfactant and (*c*) XRD pattern of a Sn–TiO_2 sample.

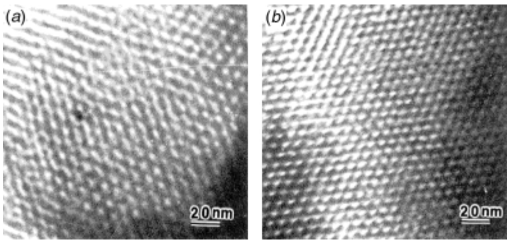

Fig. 2 TEM images of (*a*) as-synthesized (aged at 50 °C for 1 week) and (*b*) as-calcined (at 500 °C in air for 1 h) TiO_2 samples prepared using Pluronic 103 as surfactant.

Shown in Fig. 1 are small-angle XRD patterns of TiO_2 powder samples prepared using a tri-block polymer surfactant (Pluronic 103). The XRD pattern of the as-synthesized sample, Fig. 1(*a*), implies that the surfactant molecules were organized into a hexagonal superstructure after being aged at 50 °C for one week. In addition to the major peak at about 1° due to the (100) reflection, which corresponds to a *d*-spacing of 8.4 nm, small peaks due to the (110) and (200) reflections are also observable. The XRD pattern of the as-calcined sample, Fig. 1(*b*), indicates that the mesoporous structure was retained during the removal of the surfactant by calcination at 500 °C in air for 1 h, although the superstructure had contracted slightly as evidenced by a slight shift of the XRD peaks toward larger angle. The corresponding *d*-spacing was reduced from 8.4 nm for the as-synthesized sample to about 7.9 nm for the as-calcined sample. Shown in Fig. 1(*c*) is a small-angle XRD pattern of a Sn–TiO_2 sample, which is nearly identical to the XRD pattern of the as-synthesized TiO_2 shown in Fig. 1(*b*), implying that the periodicity of the mesoporous TiO_2 remain unchanged during the incorporation of tin compounds into the mesoporous TiO_2 and the reduction of tin oxide to tin metal.

Shown in Fig. 2 are TEM images of the as-synthesized and as-calcined samples. The periodicities of the mesoporous superstructure as determined from the TEM images are consistent with those determined from XRD analysis. The corresponding pore sizes are about 7.6 and 6.9 nm, respectively. The N_2 adsorption isotherms of the as-synthesized and as-calcined TiO_2 powder are shown in Fig. 3(*a*). Both adsorption isotherm curves have a well-defined step for the relative pressure P_s/P_0 ranging from 0.6 to 0.8, a characteristic of the filling of the framework-confined mesoporous, suggesting that both as-synthesized and as-calcined samples are mesoporous. However, the calculated BET surface area was increased from 203 $m^2\ g^{-1}$ for the as-synthesized sample to 603 $m^2\ g^{-1}$ for the as-calcined sample, indicating that the gas-accessible surface area was dramatically increased after the surfactant was removed. Further, the average pore size in the as-calcined mesoporous superstructure is about 6.9 nm with a narrow size distribution, as shown in the insert in Fig. 3(*a*).

After the incorporation of tin compound into the pores of the mesoporous TiO_2, the surface area and pore size were reduced to 441 $m^2\ g^{-1}$ and 6 nm, respectively, as determined from the absorption isotherm and pore size distribution data shown in Fig. 3(*b*). This implies that the tin compound was formed inside the pores of the mesoporous TiO_2, an ideal configuration of a

DOI: 10.1039/b007687m

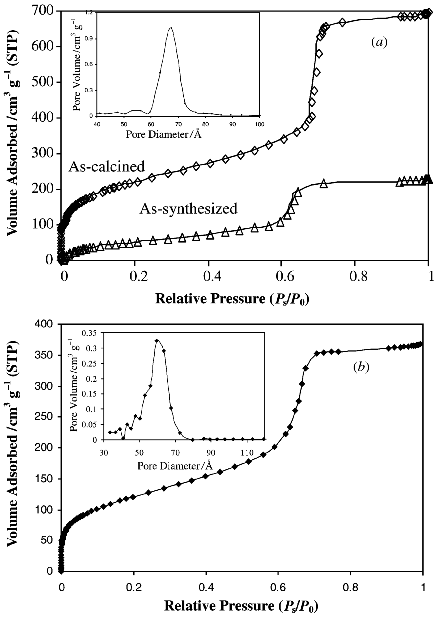

Fig. 3 (*a*) Nitrogen isotherm plots of as-synthesized (aged at 50 °C for 1 week) and as-calcined (at 500 °C in air for 1 h) TiO_2 samples prepared using Pluronic 103 as surfactant (the insert curve is the pore size distribution for the as-calcined TiO_2 sample calculated from the BET curve); (*b*) nitrogen isotherm plots of a Sn–TiO_2 composite sample (the insert curve is the pore size distribution for the composite calculated from the BET curve).

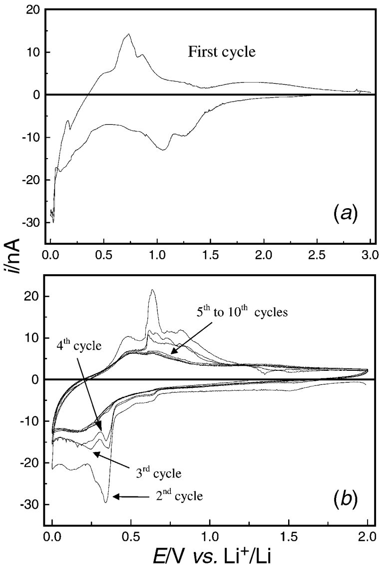

Fig. 4 Cyclic voltammograms of a mesoporous Sn–TiO_2 composite as studied using a powder microelectrode: (*a*) the cycle 1; (*b*) the 2 to 10 cycles. The potential sweep rate was 0.5 mV s^{-1}.

composite electrode for lithium batteries with desired structural stability.

Shown in Fig. 4 are the first several cyclic voltammograms of a mesoporous Sn–TiO_2 composite electrode as studied using a powder microelectrode. Clearly, the CV curve for the first cycle is very different from those commonly observed for most tin-based composite electrodes.[18] It is noted that there is no cathodic peak at 0.85 V (or 2.6 V), corresponding to electrochemical reduction of SnO or SnO_2,[18] indicating that most tin oxides had been chemically reduced to tin metal in the mesocomposite during the exposure to hydrogen. However, there are two small reduction peaks between 1 and 1.5 V in the first cycle, which disappeared after the first cycle. Several pairs of redox peaks appear in the voltammograms after the second cycle. The peak currents decreased during the first few cycles but remained relatively constant later on, as shown in Fig. 4(*b*). There was little change from 5th to 10th cycle, implying that the composite electrode may have good cycleability. Long-term cycling behavior of the composite electrode is still under investigation using constant current charge–discharge cycling test and will be reported in the near future.

In a typical preparation, 10 g titanium butoxide was dissolved in 20 ml absolute ethanol and 2.92 ml acetylacetone at room temperature before 10 ml distilled water was added, followed by stirring for another 2–3 h. In a separate beaker, 5 g Pluronic 103 was dissolved in 20 ml ethanol and 100 ml 2 M HCl solution. This surfactant solution was then slowly added to the titanium butoxide solution. The resulting solution was subsequently kept at 50 °C with continuous stirring for one week. The obtained solid product was washed and centrifuged three times using distilled water and then dried at 60 °C for 24 h and 120 °C for 5 d. The dried powder was fired at 500 °C for 1 h in air using an alumina boat to remove the surfactant.

To incorporate Sn into the pores of the mesoporous TiO_2, $SnCl_4$ was dissolved in water, to which NH_3(aq) was added to ensure all Sn^{4+} was hydrolyzed and precipitated. The solid product was washed and centrifuged three times using distilled water and was then dissolved in nitric acid to obtain a solution containing Sn^{4+}. The mesoporous TiO_2 powder was then immersed in the solution containing Sn^{4+} for a few days. The resulting powder was obtained after drying at 80 °C for one day and at 120 °C for another day, followed by reduction at 300 °C for 24 h in a hydrogen atmosphere.

The electrochemical properties of the mesoporous Sn–SiO_2 electrode were studied in 1 M $LiN(SO_2CF_3)_2$/EC+DMC electrolyte solution using a powder microelectrode[19] technique.

We gratefully acknowledge the support of this research by the National Science Foundation (under Grant No. CTS-9819850) and the Caleb Corporation.

Notes and references

1 C. T. Kresge, M. E. Leonowicz, W. J. Roth, J. C. Vartuli and J. S. Beck, *Nature*, 1992, **359**, 710.
2 J. S. Beck, J. C. Vartuli, W. J. Roth, M. E. Leonowicz, C. T. Kresge, K. D. Schmitt, C. T-W. Chu, D. H. Olson, E. W. Sheppard, S. B. Mccullen, J. B. Higgins and J. L. Schlenker, *J. Am. Chem. Soc.*, 1992, **114**, 10 834.
3 A. Sayari, *Chem. Mater.*, 1996, **8**, 1840.
4 Q. Huo, R. Leon, P. M. Petroff and G. D. Stucky, *Science*, 1995, **268**, 1324.
5 Q. Huo, D. I. Margolese, U. Ciesla, D. G. Demuth, P. Feng, T. E. Gier, P. Sieger, A. Firouzi, B. F. Chmelka, F. Schuth and G. D. Stucky, *Chem. Mater.*, 1994, **6**, 1176.
6 A. Monnier, F. Schüth, Q. Huo, D. Kumar, D. Margoless, R. S. Maxwell, G. D. Stucky, M. Krishnamurty, P. Petroff, A. Firouzi, M. Janicke and B. F. Chmelka, *Science*, 1993, **261**, 1299.
7 U. Ciesla, S. Schacht, G. Stucky, K. Unger and F. Schüth, *Angew. Chem., Int. Ed. Engl.*, 1996, **35**, 541.
8 U. Ciesla, M. Fröba, G. Stucky and F. Schüth, *Chem. Mater.*, 1999, **11**, 227.
9 M. Fröba and O. Muth, *Adv. Mater.*, 1999, **11**, 564.
10 Z. R. Tian, W. Tong, J. Y. Wang, N. G. Duan, V. V. Krishnan and S. L. Suib, *Science*, 1997, **276**, 926.
11 M. Thieme and F. Schüth, *Microporous Mesoporous Mater.*, 1999, **27**, 193.
12 V. Luca, D. J. Maclachlam, J. M. Hook and R. Whiters, *Chem. Mater.*, 1995, **7**, 2220.
13 D. M. Antonelli and J. Y. Ying, *Angew. Chem., Int. Ed. Engl.*, 1995, **34**, 2014; *Chem. Mater.*, 1996, **8**, 874; D. M. Antonelli, A. Nakahira and J. Y. Ying, *Inorg. Chem.*, 1996, **35**, 426.
14 D. Zhao, J. Feng, Q. Huo, N. Melosh, G. Fredrickson, B. Chmelka and G. D. Stucky, *Science*, 1998, **279**, 548.
15 P. Yang, D. Zhao, D. I. Margolese, B. F. Chemelka and G. D. Stucky, *Nature*, 1998, **396**, 152.
16 D. M. Antonelli, *Microporous Mesoporous Mater.*, 1999, **30**, 315.
17 R. A. Huggins, *Solid State Ionics*, 1998, **113–115**, 57.
18 S. Machill, T. Shodai, Y. Sakuraai and J. Yamaki, *J. Power Sources*, 1998, **73**, 216.
19 C. S. Cha, C. M. Li, H. X. Yang and P. F. Liu, *J. Electroanal. Chem.*, 1994, **368**, 47.